To be submitted to
Lettere al Nuovo Cimento

COMITATO NAZIONALE PER L'ENERGIA NUCLEARE
Laboratori Nazionali di Frascati

LNF-74/46(P)
5 Agosto 1974

F. Balestra, R. Barbini, L. Busso, R. Garfagnini,
C. Guaraldo, G. Piragino and R. Scrimaglio:

(π^-, ^{12}C) ELASTIC BACKWARD SCATTERING.

Servizio Documentazione
dei Laboratori Nazionali di Frascati del CNEN
Casella Postale 70 - Frascati (Roma)

Laboratori Nazionali di Frascati del CNEN
Servizio Documentazione

LNF-74/46(P)
5 Agosto 1974

F. Balestra(x), R. Barbini, L. Busso(x), R. Garfagnini(x), C. Guaraldo, G. Piragino(x) and R. Scrimaglio: (π^-, ^{12}C) ELASTIC BACKWARD SCATTERING.

SUMMARY. -

Measurements have been made of the differential cross section in the process (π^-, ^{12}C) with incident energies ranging from 60 up to 90 MeV and in the angular region 160^o-180^o.

The experimental apparatus was a magnetic spectrometer with a streamer chamber filled with helium at atmospheric pressure used as particle's visualizer. In a phase shift analysis of the (π^-, ^{12}C) scattering our backward cross sections can profitably help for choosing the correct set of fitting phase shifts.

RIASSUNTO. -

Sono state eseguite misure della sezione d'urto differenziale nel processo (π^-, ^{12}C) con energie incidenti da 60 sino a 90 MeV e nella regione angolare 160^o-180^o.

Come apparato sperimentale è stato usato uno spettrometro magnetico con una camera a streamer a elio a pressione atmosferica usata come visualizzatore di particelle. In un'analisi in fase della diffusione (π^-, ^{12}C) i nostri dati a grande angolo possono dare utili informazioni per la scelta del giusto insieme di sfasamenti tra i vari possibili che riproducono i risultati sperimentali.

(x) - Istituto di Fisica Generale dell'Università di Torino, and Istituto Nazionale di Fisica Nucleare, Sezione di Torino.

I. - INTRODUCTION -

In the comparision between theory and experiments on the pion scattering by light nuclei ($A \lesssim 20$) up to 280 MeV three separate energy region must be distinguished.

1) Low energies (≤ 40 MeV). A velocity-dependent (Kisslinger) potential[1] turns out to be rather well suited for explaining experimental data even at large angles, due to the smallness of πN scattering amplitudes and the domination of single scattering[2, 3].

2) Intermediate energies ($40 \div 120$ MeV). The Kisslinger-type potential fails to fit data for scattering angles larger than 60 deg about[4]. Other models such as the "effective-raius" and "matter-radius"[2] ones don't either show a better behaviour.

3) Energies in the region of the (3, 3) resonance: $120 \leq T_\pi \leq 280$ MeV. Data can be more reasonably explained in terms of a Glauber-type analysis[5] or of even more simple optical models (viz. the "effective radius" model). Such models however feels the effects of their high energy derivation and rapidly become unsuccessful whenever energies are not so large to allow for neglecting the nuclear structure contribution.

In the intermediate energy region a phase shift analysis[6] carried out by adjusting iteratively the parameters of the various partial waves can yield a satisfactory interpretation of the experimental results. In this case, however, different sets of phase shifts fit equally well the existing experimental data up to an angle of 120°, while they deviate at larger angles: at 180° this difference may reach two orders of magnitude (see fig. 3). Therefore large angle and backward scattering cross sections must be known in order to be able to choose the correct set of phase shifts.

As a conclusion, elastic (and inelastic) large angle scattering data of pions on nuclei can provide essential informations for a broad energy region ($20 \div 150$ MeV), on the reliability of the various pion-nucleus interaction models proposed up to now. The ^{12}C nucleus is a convenient target for at least three reasons: the best available data of scattering up to 140 deg have been obtained for this nucleus, it shows a convenient separation among the first nuclear levels and moreover only few cloud chamber data[7, 8] with poor resolution exist for large angle ($> 140^\circ$) π^--^{12}C scattering.

In this paper we present preliminary data on (π^-, ^{12}C) elastic scattering in two angular bins, 160°-170° and 170°-180°, and for four incident pion energies: 60 ± 5 MeV; 70 ± 5 MeV, 80 ± 5 MeV, 90 ± 5 MeV.

2. - THE EXPERIMENTAL APPARATUS -

The experimental apparatus we used is shown in Fig. 1 and has been described in detail in ref. (9, 10). It is a magnetic spectrometer with streamer chamber for identifying scattering events by detecting both the incident and scattered pion tracks. The streamer chamber, is filled with helium at atmospheric pressure and contaminated by small amounts ($< .05\%$) of nitrogen and xenon. A fourteen stage pulse generator of the Arkadiev-Marx type, was used for firing the high voltage pulse on the chamber. The photographs are taken by two cameras with the axes parallel to the magnetic field.

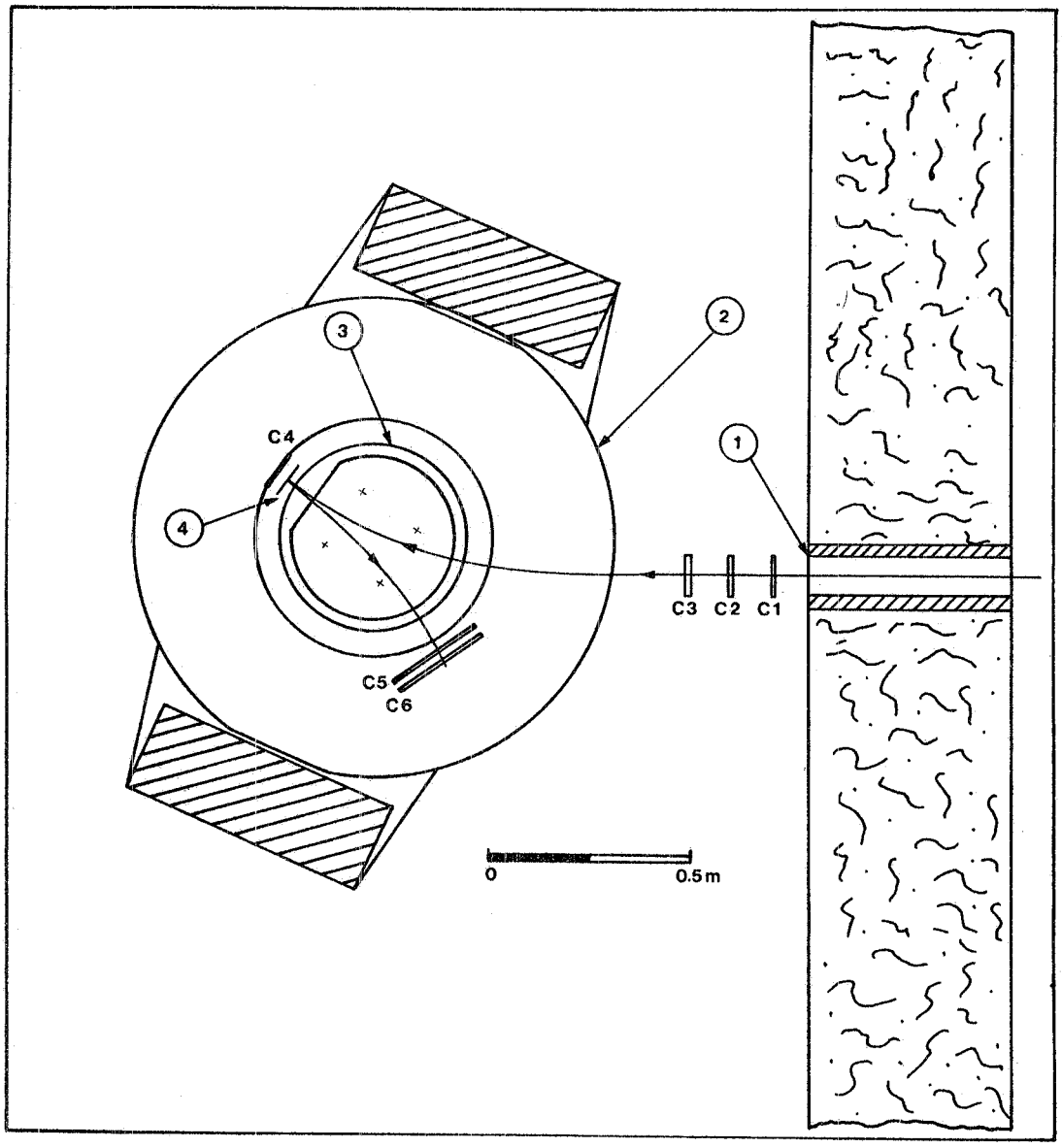

FIG. 1 - Layout of the experimental apparatus. 1) Collimator (10x4) cm^2; 2) Magnet; 3) Streamer chamber; 4) Target; 5) C_1 to C_6 counters.

The odoscope of thin scintillation counters $C_1C_2C_3C_4$ defines the geometry (100 x 40 mm^2) and the number of pions deflected by the magnet and impinging on the experimental target. We used a carbon target. We used a carbon target (50 x 100 x 3 mm^3), of measured density, 1,86 g/cm^3, located 3 cm before the counter C_4. Pions scattered in the backward direction by the target are deflected with an opposite curvature by the magnetic field and are counted by the coincidence $C_1C_2C_3C_4C_5C_6$. The anticoincidence C_4 excludes those particles which have interacted out of the target. The coincidence triggers the high-voltage pulse on the streamer chamber and the command circuits of the cameras, thus allowing to photograph the scattering event.

The resolution of the apparatus is a function of a number of parameters: the track's lenght in the streamer chamber, the number of points measured along the track, the uncertainty of the measured points and the applied magnetic field, which directly affects the length of the curvature radius.

We used a magnetic field of 5 KG, which allows for a R.M.S. momentum resolution around 1%, for a track length of 28 cm, 15 points measured on it, an uncertainty of $\pm$ 0.2 mm in locating the point and for curvature radii up to 1200 mm.

By means of a Montecarlo calculation which simulates both the incident pion beam and the scattering (elastic and inelastic) events, the detection efficiency of the apparatus (and therefore the effective solid angle) has been evaluated as a function of the incident pion energy, the scattered energy and the scattering angle.

The Montecarlo distributions of particles on the target and on the detectors C_5C_6 have been compared with the experimental ones obtained by measuring tracks on the films and the agreement turned out to be very good, within the statistical errors.

3. - THE PION BEAM -

The pion beam used in this experiment is the one available at the LEALE Laboratory of LNF[11]. The e^- beam of the Frascati Linac impinges upon a tungsten radiator giving rise to a bremsstrahlung secondary beam which in turn photoproduces positive and negative pions by interacting with a graphite target. Pions are collected at 90 deg. by a magnet with a large momentum acceptance ($\pm$ 20%). Tungsten and graphite are separated by a distance of 35 cm which is occupied by a sweeping magnet. The magnet deflects downward, electrons which otherwise should reach the graphite target and contaminate the pion beam. The pion

beam intensity can be charged by varying the tungsten target thickness; the pion beam central energy can be simply changed by tuning the magnetic field of the collecting magnet. A set of adjustable slits placed on the focal plane of this magnet defines the momentum band of the pion beam actually used in the experiment.

In this measurement we accepted a beam with a $\pm$ 15% momentum distribution around the central value, in order to carry out simultaneously measurements for more than one incident energy. The production point of pions is 8.75 m afar from the experimental target so that the actual central pion energy at the target position depends on energy losses suffered by particles along their path, in the interaction with air, counters, streamer chamber's walls, etc.

4. - EXPERIMENTAL PROCEDURE -

The nominal π^- beam central energy was 88 MeV, corresponding 77.5 MeV at the target position; the intensity of pions incident on the target was around 10^2 π^-/sec[12] and gave rise to about 0,05 sec streamer chamber's triggers (events + background).

The pion dose has been corrected for the counters' efficiences (> 90%) and for contaminations of the pion beam due to e^- and to decay μ^-. The e^- contamination has been measured by a CO_2 gas Cerenkov counter and resulted to be account 2%. The μ^- contamination has been measured by means of the integral and differential range technique and was found to be $\approx$ 8%.

This technique allowed also for experimentally measuring the energy distribution of pions on target, whose central value resulted in very good agreement with the one measured in the streamer chamber and to the one calculated in terms of the energy losses along the pions' path. The probability for the scattered pions to be lost as a consequence of decay in the distance between the target and the final counters (C_5C_6) has been evaluated to be negligible. Negligible as well is to be considered the e^- and μ^- scattering contribution to the measured events.

The initial pictures of each run have been exposed by triggering the streamer chamber with the $C_1C_2C_3C_4$ coincidence pulse in order to reconstruct the momentum spectrum of the incident pion beam. During each run the stabilities of magnetic fields have been maintained within 1‰, and the energy spectrum of the primary e^- beam within less than 5%.

The two stereo view of each event have been measured with the help of a semiautomatic image plane digitizer to reconstruct the tracks in space.

In doubtful cases the same tracks have been measured repeatedly and the errors have been drawn by the resulting experimental distributions. The events' vertex must obviously lie in the volume of the target. Errors in the reconstruction of tracks and radii affect the location of the vertex. However, taking into account such errors as well, the separation between events occurred in the target and in the counter C_4 appears to be sufficiently unambiguous. In this way events which have originated in the counter and not previously rejected by the anticoincidence C_4 (inefficiency $\simeq$ 10%) can be eliminated. The reconstructed scattering angle is neglibly affected either by reconstruction errors ($\pm$ 0.5°) and by the multiple scattering in the target. A computer routine (LEVEL) with takes advantage of the angular and energy informations (with their errors) assigns the events to the elastic channel or to inelastic ones by evaluating the normalized probability for the event to belong to each of the above processes. The program takes also properly in account the average ionization energy losses of both the incoming and scattered pions in the target. After this processing, events are corrected further on for the effective solid angle factor.

The incident dose related to each energy interval is evaluated by extracting from the incident pion energy spectrum (taken at the beginning of the run) the fraction of pions falling in the interval in question.

5. - RESULTS AND DISCUSSION -

The cross sections we obtained are shown in Table I. The energy intervals covered by these measurements are 60 $\pm$ 5 MeV, 70 $\pm$ 5 MeV, 80 $\pm$ 5 MeV, 90 $\pm$ 5 MeV; data have been divided in two 10° angular bins: 160°÷170° and 170°÷180°. The errors quoted are only statistical.

TABLE I - (π^-, ^{12}C) Backward scattering differential elastic cross section (mb/sr).

T_π (MeV) \ θ	160°-170°	170°-180°
60 $\pm$ 5	3.1 $\pm$ 1.59	2.38 $\pm$ 0.95
70 $\pm$ 5	1.04 $\pm$ 0.49	1.74 $\pm$ 0.41
80 $\pm$ 5	0.73 $\pm$ 0.28	0.42 $\pm$ 0.21
90 $\pm$ 5	0.75 $\pm$ 0.41	0.70 $\pm$ 0.49

In the near future we will extend the angular range (140^{o} to 180^{o}), the incident energy values (down to 30 MeV) and the statistics.

In fig. 2 our data are plotted together with the exsisting scattering data[13, 14, 4] up to 120^{o} at the energies involved in this work.

On the basis of the experimental results obtained we can draw the following conclusions:

1) The 70 MeV data show a different behaviour between 160^{o} and 180^{o} in comparison with the 80 and 90 MeV data. This fact becomes more evident if we group our data in the narrower energy bin $70 \div 75$ MeV.

2) It is not clear to which extent our 80 MeV elastic cross section near 180^{o} can be reproduced by a Kisslinger model, either with theoretical or with best-fit parameters, according to the calculations of Auerbach et al.[4] for the (π^{-}, ^{12}C) data of Baker et al.[13] up to 120^{o}. Moreover, also an "effective radius" model is not likely to match our large angle data (see fig. 4).

3) Nevertheless, our data provide sufficient information for choosing one of the phase-shifts sets proposed by Beiner and Huguenin[6] in their phenomenological interpretation of pion-nucleus scattering (see fig. 3).

4) Anyhow, to link correctly forward and backward scattering data we need further measurements between 140^{o} and 160^{o} after which an ultimate answer on the reliability of the various models should be at hand.

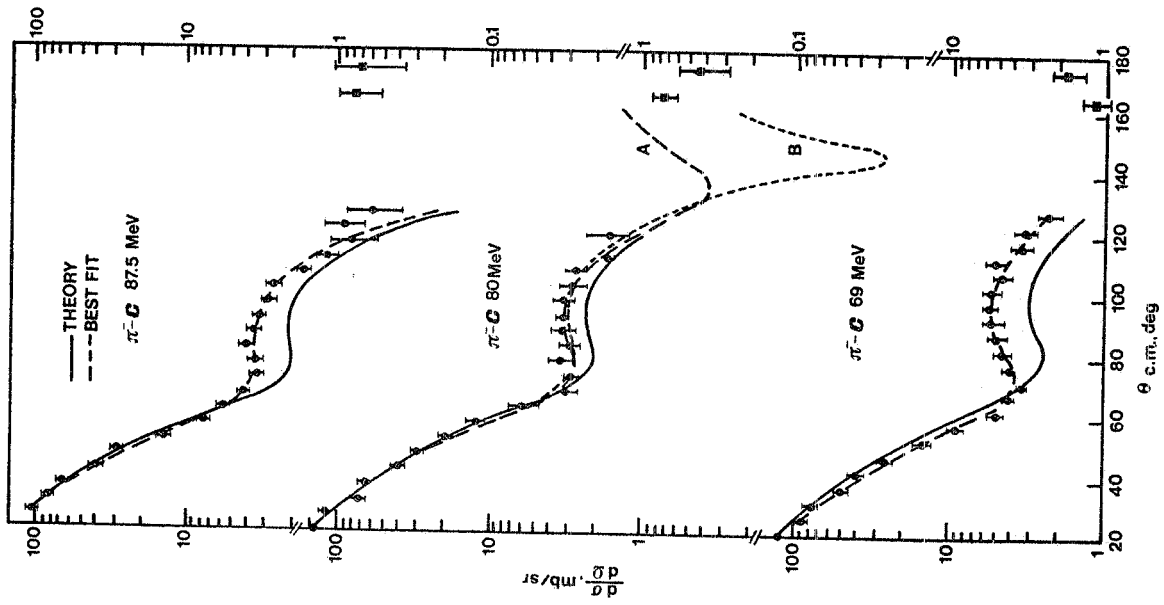

FIG. 2 - π^- - Carbon elastic scattering at 69, 80 and 87.5 MeV. The 80 MeV experimental data up to 120° are those of Baker et al. (ref. 13); the 69 and 87.5 data were obtained by Edelstein et al. (ref. 14). Our large angle data are also plotted in this figure.
The curves give cross sections calculated by Auerbach et al. (Ref. 4). Solid curves have been calculated by inserting in the optical Kisslinger potential theoretical parameters derived by π-nucleon phase shifts, and using modified Gaussian nuclear densities. Dashed curves instead give the best fits obtained by varying both the potential's and the Gaussian nuclear density's parameters. For the 80 MeV data the best fit Gaussian cross section is not plotted, and curves A and B refer to two different sets of parameters for an assumed Saxon-Woods nuclear density.

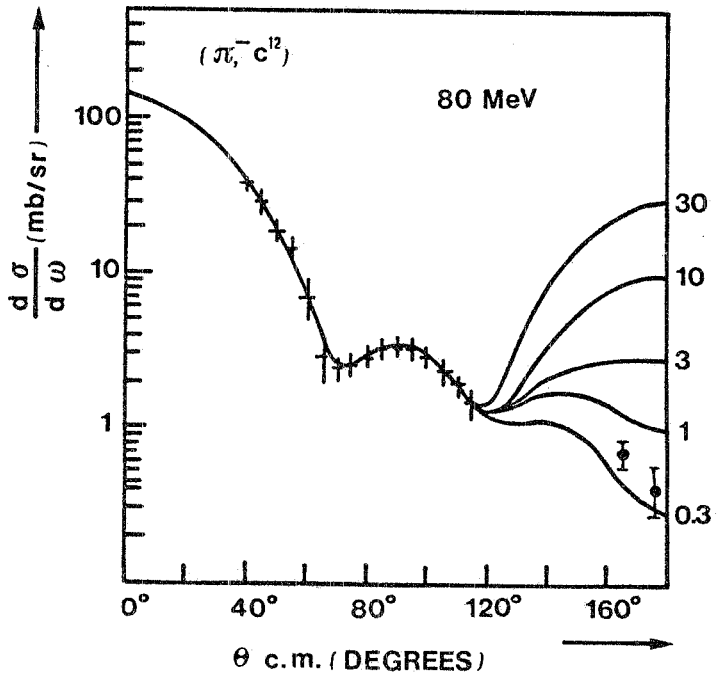

FIG. 3 - π^- - Carbon elastic scattering at 80 MeV. The experimental data up to 120° are those of Baker et al. (ref. 13). Our large angle data are also plotted in this figure. Solid curves are calculated by Beiner et al. (ref. 6) in terms of a phase shifts analysis. Different sets of phase shifts can equally well reproduce experimental data up to 120°, but give very different results at backward angles, where they give cross sections ranging from .3 to 30 mb/sr. Our experimental data should provide enough information for choosing the correct set of phase shifts.

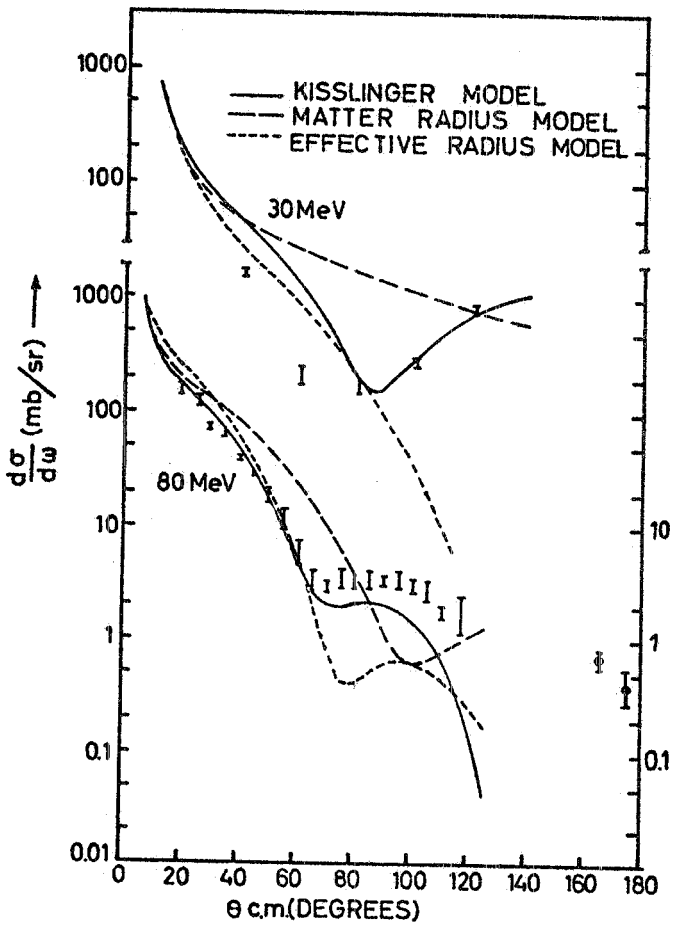

FIG. 4 - π^- Carbon elastic scattering at 80 MeV. The experimental data up to 120° are those of Baker et al. (Ref. 13). Our large angle data are also plotted in this figure. The curves give cross sections calculated by Silbar et al. (Ref. 2). The solid curve refer to an assumed Kisslinger potential with parameters obtained from π-Nucleon phase shifts. Dashed curves are related to the "matter radius" and to the "effective radius" models respectively. A modified Gaussian nuclear density has been used throughout.

REFERENCES AND FOOTNOTES -

(1) - L.S. Kisslinger, Phys. Rev. 98, 761 (1955); E.H. Auerbach, D. M. Fleming and M.M. Sternheim, Phys. Rev. 162, 1683 (1967); M.M. Sternheim and E.H. Auerbach, Phys. Rev. Lett. 25, 1500 (1970); J.P. Dedonder, Nucl. Phys. A 174, 251 (1971), and A 180, 472 (1972).

(2) - M. Silbar and M.M. Sternheim, Phys. Rev. Letters.

(3) - J.F. Marshall, M.E. Nordberg Jr. and R.L. Burman, Phys. Rev. C 1, 1685 (1970).

(4) - E.H. Auerbach, D.M. Fleming and M.M. Sternheim, Ref. 1.

(5) - R.J. Glauber: Lectures in Theoretical Physics, Vol. 1 (New York, 1959); C. Schmit, Lett. Nuovo Cimento, 4, 454 (1970); C. Wilkin, Lett. Nuovo Cimento 4, 491 (1970).

(6) - J. Beiner and Huguenin, Helv. Phys. Acta 42, 550 (1969); J. Beiner, Nucl. Phys. B 53, 349 (1973).

(7) - H. Byfield, J. Kessler and L.M. Lederman, Phys. Rev. 86, 17 (1952); J.O. Kessler and L.M. Lederman, Phys. Rev. 94, 689 (1954).

(8) - V.P. Dzhelepov et al. Sov. Phys. JEPT 4, 864 (1957).

(9) - F. Balestra, R. Barbini, L. Busso, I.V. Falomkin, R. Garfagnini, C. Guaraldo, M.M. Kulyukin, G. Piragino, R. Scrimaglio and Yu. A. Shcherbakov, Nucl. Instr. and Meth. 119, 347 (1974).

(10) - F. Balestra, R. Barbini, L. Busso, I.V. Falomkin, R. Garfagnini, C. Guaraldo, M.M. Kulyukin, G. Piragino, R. Scrimaglio and Yu. A. Shcherbakov, LNF-74/45 (1974) and submitted to Nucl. Instr. and Meth.

(11) - R. Scrimaglio, Frascati Report LNF-68/14(Int.) (1968); R. Barbini, C. Guaraldo and R. Scrimaglio, LNF-68/15(Int.) (1968); R. Barbini, C. Guaraldo, P. Picozza, C. Schaerf and R. Scrimaglio, LNF-70/5(Int.) (1970); R. Barbini, S. Faini, C. Guaraldo, P. Picozza, C. Schaerf and R. Scrimaglio, Nuclear Instr. and Meth. 105, 515 (1972); R. Barbini, C. Guaraldo, C. Schaerf and R. Scrimaglio, Nuclear Instr. and Meth. 115, 85 (1974); R. Barbini, C. Guaraldo, C. Schaerf and R. Scrimaglio, Nuclear Instr. and Meth. 119, 35 (1974); R. Barbini, C. Guaraldo and R. Scrimaglio, LNF-74/33(P) (1974), and submitted to Nuclear Instr. and Meth.

(12) - The corresponding intensity on the focal plane of the collecting magnet is $\approx 5 \cdot 10^4$ π^-/sec: it must be noticed, however, that the highest available intensity of LEALE pion beam is of the order of 10^6 π^-/sec.

(13) - W.F. Baker, J. Rainwater and R.E. Williams, Phys. Rev. 112, 1763 (1958).

(14) - R.M. Edelstein, W.F. Baker and J. Rainwater, Phys. Rev. 122, 252 (1961).